Reflectance imaging by fiber bundle endoscope: Vertical reconstruction by multipositional illumination

Yoriko Ando, Kowa Koida, Hirohito Sawahata, Takashi Sakurai, Mitsuo Natsume, Takeshi Kawano, and Rika Numano

Citation: AIP Conference Proceedings **1709**, 020009 (2016); doi: 10.1063/1.4941208
View online: http://dx.doi.org/10.1063/1.4941208
View Table of Contents: http://scitation.aip.org/content/aip/proceeding/aipcp/1709?ver=pdfcov
Published by the AIP Publishing

Reflectance Imaging by Fiber Bundle Endoscope: Vertical Reconstruction by Multipositional Illumination

Yoriko Ando[a*], Kowa Koida[a,b], Hirohito Sawahata[c], Takashi Sakurai[d], Mitsuo Natsume[e], Takeshi Kawano[c] and Rika Numano[a,f*]

[a] *Electronics-Inspired Interdisciplinary Research Institute (EIIRIS), Toyohashi University of Technology, 1-1 Hibarigaoka, Tempaku-cho, Toyohashi, 441-8580, Japan*

[b] *Department of Computer Science and Engineering, Toyohashi University of Technology*

[c] *Department of Electrical and Electronic Information Engineering, Toyohashi University of Technology*

[d] *Juntendo University, 2-1-1 Hongo, Bunkyo-ku, Tokyo, 113-8421, Japan*

[e] *Denkosha, 95 Oroshihonn-machi, Minami-ku, Hamamatsushi, 432-8055, Japan*

[f] *Department of Environmental and Life Science, Toyohashi University of Technology*

*Email: ando@eiiris.tut.ac.jp, numano@eiiris.tut.ac.jp

Abstract. Fiber bundles for imaging internal organs with minimum physical damage have been increasingly developed for both basic life sciences and clinical applications. Reflectance imaging is possible using fiber bundles for detecting the intrinsic optical contrast of blood vessels and tissue structure. The placement of an illumination source adjacent to imaging optics causes scattered light from deeper tissue layers to illuminate superficial tissues and results in a reflectance image. However, it does not have focal capacity and lacks depth resolution. In this study, we performed spatial analysis for the vertical reconstruction of *in vivo* tissues using a multipositional illumination scheme. The observed image corresponded to the "shadow" of a target object. When we manipulated the location of illumination, the shadow moved horizontally depending on the depth of the target. We used this horizontal displacement as a cue and successfully performed the vertical reconstruction of mouse brain blood vessels.

Keywords: Reflectance imaging, Endoscopy, Fiber optics

The Irago Conference 2015
AIP Conf. Proc. 1709, 020009-1–020009-13; doi: 10.1063/1.4941208

INTRODUCTION

Novel optical technologies for imaging the internal body with minimal invasion have emerged in biomedical research and endomicroscopy, in particular, has become an important tool, producing high-resolution images with a wide field-of view. For imaging areas within living organisms that are inaccessible to conventional optical imaging, fiber bundle optics that work by insertion of a miniature tip with minimal physical damage have been developed [1-4]. This is comprised of individual step index fibers in a close-packed arrangement and maintains the relative arrangements of individual fibers allowing microscopic images to be produced in a pixelated form.

Fiber bundles can be used as probes for endomicroscopy and reflectance imaging is very useful for detection of the intrinsic optical contrast of blood vessels and tissue structure. It is necessary to efficiently reject back-reflections from the bundle end-faces. This problem is resolved by placing an illumination source adjacent to the imaging optics. Superficial tissue is illuminated from behind by light scattered from deeper tissue layers, and the scattered light provides a vertical illumination source, resulting in images with some similarities to a transmission microscope.

The fiber bundle without any lens system does not have focal capacity and lacks of depth resolution. The observed reflectance image corresponded to the "shadow" of the target object. The three-dimensional location information of the blood vessels and tissue was lost, and was projected onto a two-dimensional plane, the tip of the fiber bundle. However, three-dimensional information is important in a cellar-level imaging and endocytoscopy [5, 6].

In this study, we performed a spatial analysis for the vertical reconstruction of *in vivo* tissue using a multipositional illumination scheme. Manipulating the position of the illumination caused the shadow to move horizontally depending on the depth of the target (Fig. 1). We used this horizontal displacement as a cue, and successfully reconstructed the vertical position of the target. The difference in the depth of blood vessels in a mouse brain was detected by comparing each reflectance image obtained with four independent sites of illumination. The advantage of our approach is the ability to produce three-dimensional information with live images.

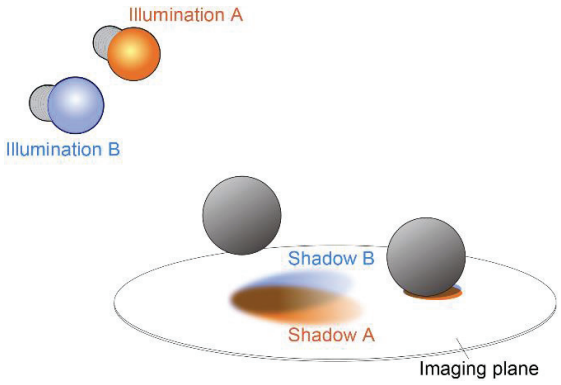

FIGURE 1. Multipositional illumination scheme. The shadow of an object changes depending on the location of illumination. It moves horizontally depending on the distance (depth) of a target.

MATERIALS AND METHODS

Animals

C57BL/6N mice (RIKEN) were maintained under controlled environmental conditions at a temperature of 22 ± 2°C, housed in cages with food and water available ad libitum under specific pathogen-free (SPF) conditions (Precision Air Processor, PAP01B, Orion), and trained to a 12:12 h light/dark cycle. The skull was ground using a dental drill (Minitor JET II, UC230). The imaging of the microvascular area was observed from above the dura layer. This study was carried out in strict accordance with the Guide for the Care and Use of Laboratory Animals from Toyohashi University of Technology. The protocol was approved by the Animal Research Committee of Toyohashi University of Technology (Permit number: DO26-6). All surgical procedures were performed under urethane anesthesia, and every effort was made to minimize suffering. The mice were immediately euthanized after the experiments.

Experimental setup of the bundled-fiber-coupled endomicroscope

The experimental setup of the fiber-bundle-coupled endomicroscope system is shown in Fig. 2(a) and consisted of an objective lens (×20, NA 0.5) and a tube lens (f = 180) optically coupled to the fiber bundle (DP-SMD002; Denkosha), and a cooled EM-CCD camera (512 × 512 pixels, 1 × 1 binning, −90 ± 5°C, iXon; Andor Technology). The focal plane of the objective lens was optically aligned with the side of the fiber bundle in contact with the target.

Figure 2(b) shows the entire face of the fiber bundle. The bundle itself was made up of 54,000 single fibers, each 1.8 μm in diameter; the distance between unit fibers was 2.4 μm, and the tip of the fiber bundle was 600 μm in diameter. High-magnification examination of the fiber bundle (Fig. 2(b)) showed individual fibers arranged in a close-packed structure. The lateral optical resolution of the fiber bundle, determined by the core-to-core distance, was 2.4 μm.

Light from white LED (for the reflectance imaging of micro beads and the OHP sheet) and a Hg lamp (C-HGFIE, Nikon) with a monochromator (UV-VIS Monochromator, SPG-120S, Shimadzu) at 436 nm (for the blood vessels) was optically coupled to twelve single-mode fibers (250 μm in diameter, CK-10, Mitsubishi Rayon) surrounded by a fiber bundle and used as the illumination light source (Fig. 2(c)). Three of the twelve single fibers were coupled as a group enabling the specimen plane to be illuminated from four individual sites (#1, #2, #3, and #4) i.e., multipositional illumination. Heat shrink tubing around the insertion point held the fiber bundle and the illumination fibers in position. The navigation of these was carried out at the xyz axis positioning stage. The tip was placed on the target. Light reflected from the target was collected by the lens system and imaged using a CCD camera. Reflectance imaging was performed at time integrals of 0.1–0.5 s. Imaging data was acquired by Solis (Andor Technology) and analyzed and processed by MATLAB (MathWorks).

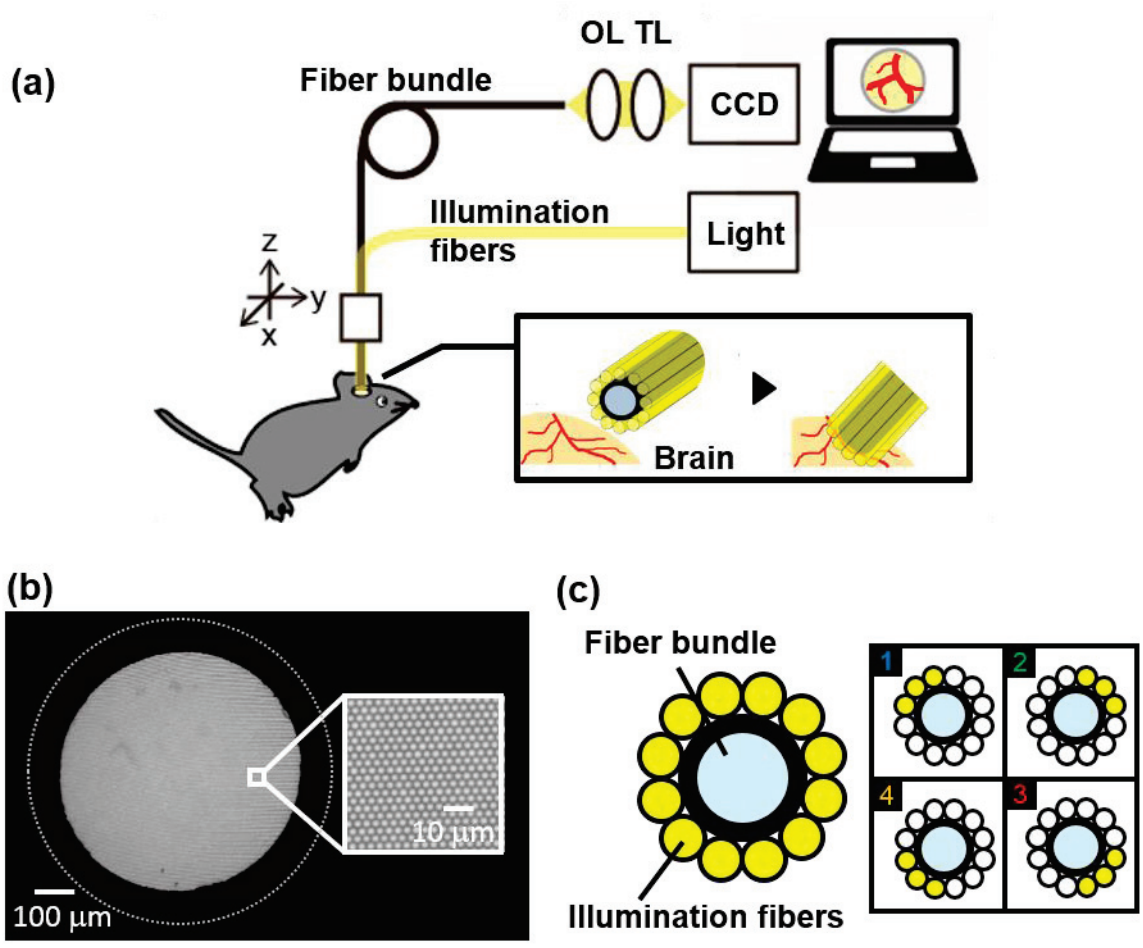

FIGURE 2. (a) Setup of the bundled-fiber-coupled endomicroscope for reflectance imaging. OL: objective lens. TL: tube lens. (b) Cross-section of the fiber bundle. (c) Multipositional illumination scheme of the bundled-fiber-coupled endomicroscope. Three of the twelve illumination fibers are grouped to provide one site of illumination. There are four illumination sites (#1 to #4).

Experiment 1: Reflectance imaging of micro beads with changing distance

Reflectance imaging of micro beads with multipositional illumination was performed with changing distance from the beads to the tip of the fiber as shown in Fig. 3(a). Micro beads of 10 μm diameter were scattered (buried) at the surface of a 0.5% agar gel in water (10–15 μm, FluoSpheres polystyrene microspheres, F8833; Molecular Probes). White-LED light optically coupled to twelve single fibers was used as the illumination light source.

From the reflectance image the center (x, y) of each bead with changing distance was obtained. In Fig. 3(b) the colored circles show the location of the micro bead in the reflectance image with each four site of illumination. The distances between centers of Illumination #1 and #3 (Shift I), and #2 and #4 (Shift II) were calculated. Illuminations #1 and #3, and #2 and #4 were combinations of the illumination placed on the opposite side (Fig. 2(c)). The average of Shift I and Shift II with changing distance was obtained. It is possible to estimate the depth of an object, located at an unknown depth, from the results of the shift value vs. distance in this experiment.

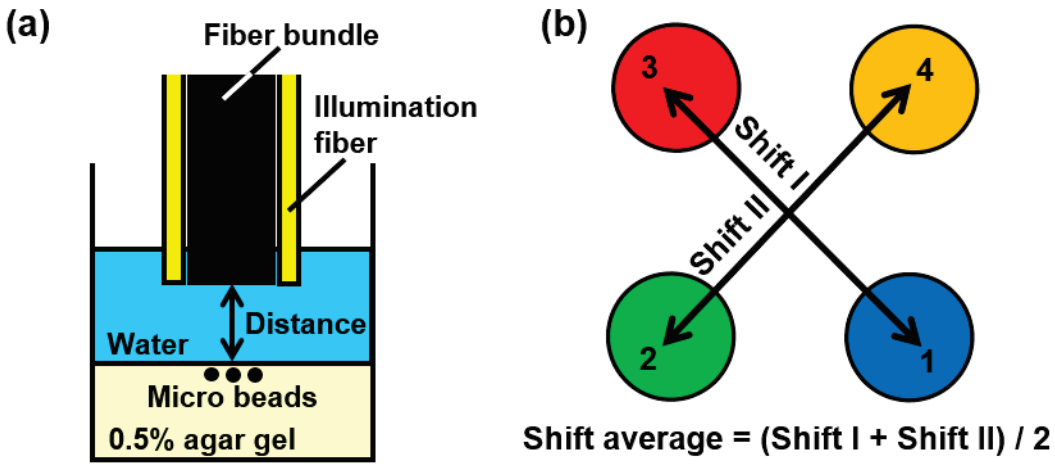

FIGURE 3. (a) Experimental setup for spatial analysis of the reflectance imaging of micro beads with multipositional illumination. (b) The calculation of the shift value of the reflectance imaging of a micro bead with multipositional illumination. Colored circles show locations of the reflectance image of the micro bead with each four illumination site. Shift I and Shift II show the distances between the centers of the reflectance images with illuminations #1 and #3, and #2 and #4 respectively. The average of Shift I and Shift II with changing the distance was calculated as the shift value.

Experiment 2: Reflectance imaging of ink-marks printed on OHP sheet

The experimental setup for the spatial analysis of reflectance imaging of ink-marks printed on a transparent film

(OHP sheet) with multipositional illumination is shown in Fig. 4. The reflectance image was obtained by a bundled-fiber-coupled endomicroscope with multipositional illumination. Ink-marks were printed on the front and back of an OHP sheet of thickness 100 μm. We performed this analysis to confirm the ability of the multipositional illumination scheme in vertical reconstruction using targets that have a known distance between them.

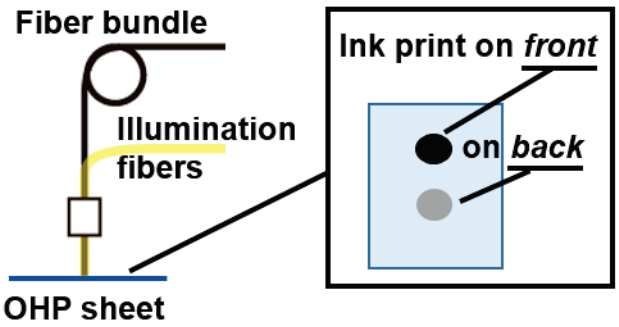

FIGURE 4. Experimental setup for spatial analysis of the reflectance imaging of ink-marks printed on an OHP sheet.

Experiment 3: Reflectance imaging of mouse brain blood vessels *in vivo*

We used illumination from a Hg lamp, at a wavelength of 436 nm through the monochromator, for the reflectance imaging of mouse brain blood vessels in order to highlight them that have strong absorption. The reflectance image was measured using the bundled-fiber-coupled endomicroscope with multipositional illumination.

Cross-correlation analysis and vertical reconstruction of the reflectance image

Cross-correlation analysis between regions of interest (ROIs) in images A and B was performed for vertical reconstruction of the target of the reflectance image. ROI in image B shifted in both x and y directions over a certain area (Fig. 5). The cross-correlation coefficient between ROIs in images A and B was calculated. When the maximum cross-correlation coefficient was obtained, the shift value of ROI in image B was calculated. The average of the shift values obtained with illumination #1 and #3, and #2 and #4 were calculated. We were able to reconstruct the vertical position and estimate the depth of the target in the reflectance imaging using the result of the shift value vs. distance in Experiment 1.

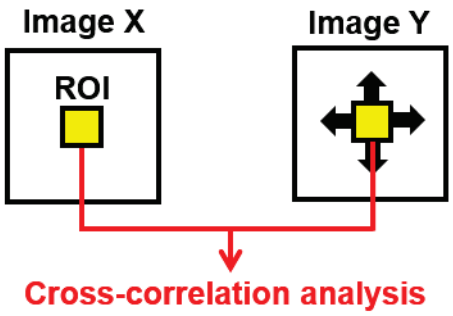

FIGURE 5. Cross-correlation analysis between ROIs in image A and image B. ROI in image B was shifted in both x and y directions. The cross-correlation coefficient between ROIs in image A and image B was calculated. When the maximum cross-correlation coefficient was obtained, the shift value of ROI in image B was calculated. The average of the shift values obtained with illumination #1 and #3 (Shift I) and #2 and #4 (Shift II) were determined, the average of these was then calculated.

RESULTS

Experiment 1: Reflectance imaging of micro beads with changing distance

Reflectance images of 10-μm beads with distances 0 μm and 300 μm at each four site of illumination (#1 to #4) were obtained as shown in Figs. 6(a). Figure 6(b) shows plots of color-filled circles of the reflectance image of the micro beads with four sites of illumination, at distances 0 μm and 300 μm. When the distance was 0 μm, the location of the reflectance images of the micro beads overlapped. On the other hand, when it was 300 μm, they separated.

The average of the shift values (Shift I and Shift II in Fig. 3(b)) with changing distance was obtained as shown in Fig. 7. The solid line represents the linear fit of the data. The shift values changed linearly depending on the distance.

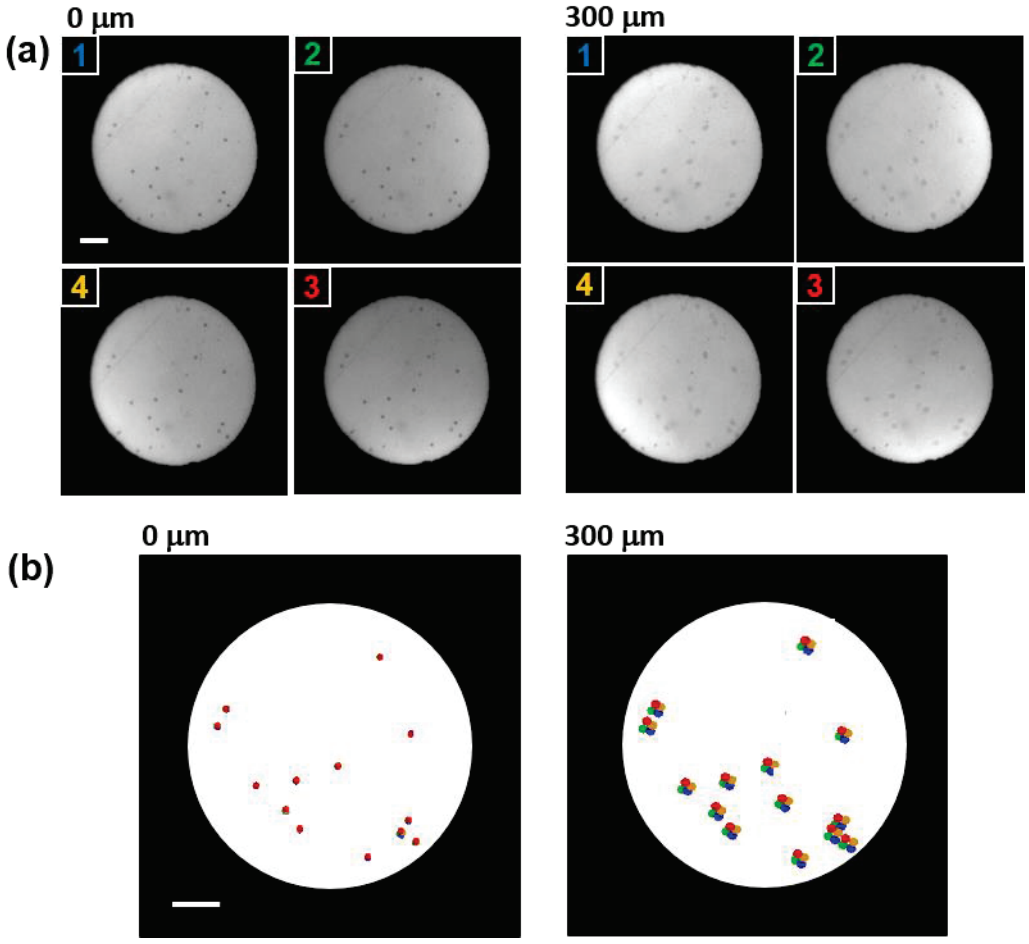

FIGURE 6. (a) Reflectance image of micro beads with changing the distance with four sites of illumination (#1 to #4) at distances 0 μm and 300 μm. (b) Plots of colored circles showing the reflectance images of micro beads at each illumination site at distances 0 μm and 300 μm from (a).

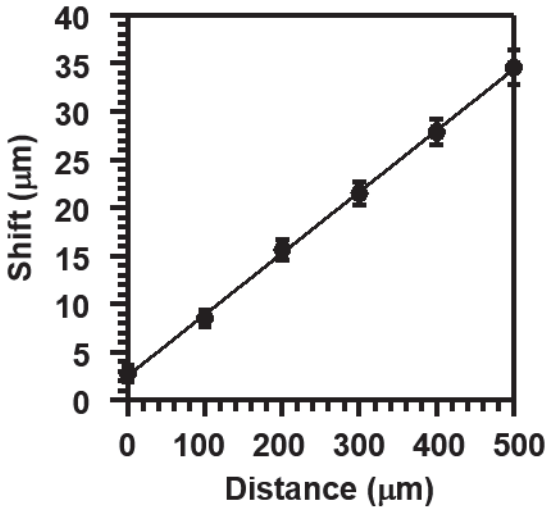

FIGURE 7. The average of the shift values (Shift I and Shift II) with changing distance.

Experiment 2: Reflectance imaging of Ink-marks printed on OHP sheet

Reflectance images of ink-marks printed on OHP sheets with multipositional illumination (#1 to #4) were obtained as shown in Fig. 8. Ink-marks on the front and back did not overlap in image 1, Fig. 8(a), or did overlap in image 2, Fig. 8(b). The size of the ROI was 104 x 104 μm^2. The average of the shift values was obtained by cross-correlation analysis (Fig. 5) and the depth calculated using the results of Experiment 1 (Fig.7); image 1 and 2, Figs. 9(a) and 9(b), respectively. The averages of the depth estimation of the ink-mark on the front and back of image 1 were −32 μm and 140 μm (thickness: 172 μm), respectively. In image 2, these were −25 μm and 114 μm (thickness: 139 μm). It became clear that the difference in depth could be detected by this analysis. On the other hand, despite the thickness of the OHP sheet being 100 μm, the depths estimated by the analysis were slightly different. Therefore, the absolute depth value could not be obtained, but the relative difference could be detected. When targets located at different depths overlapped in the reflectance image, Fig. 8(b), both analyses affected each other by the surface of separation as shown in Fig. 9(b).

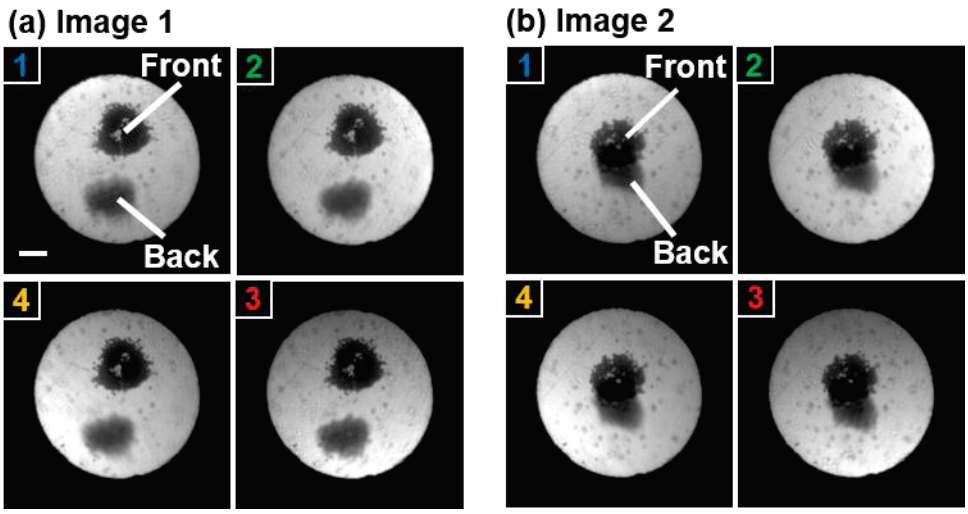

FIGURE 8. Raw reflectance image of ink-marks printed on OHP sheets with multipositional illumination (#1 to #4). Ink-marks on the front and back do not overlap in image 1 (a) and do overlap in image 2 (b).

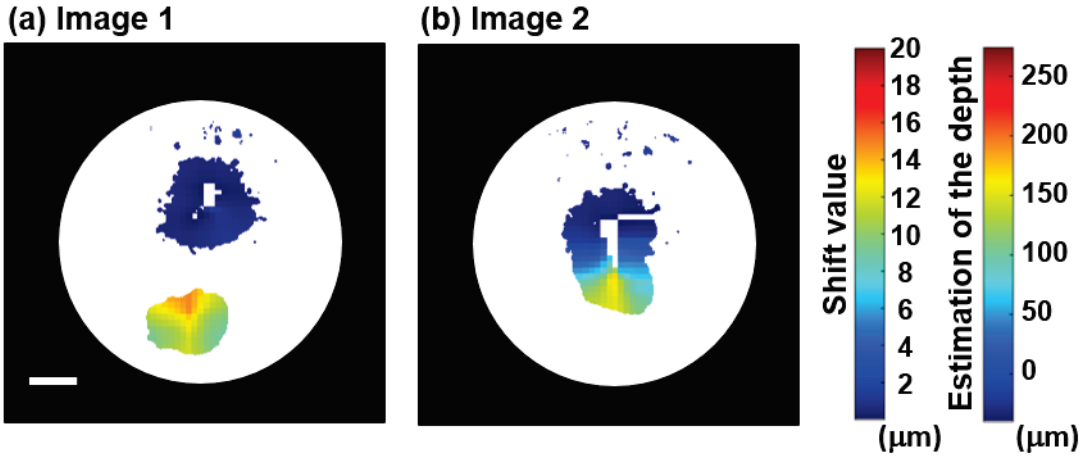

FIGURE 9. The vertical reconstruction (shift value and depth estimation) obtained by the cross-correlation analysis in image 1 Fig. 8(a) and image 2 Fig. 8(b). The color bars show the shift value and the depth estimation from the result of Experiment 1.

Reflectance imaging of mouse brain blood vessels *in vivo*

Figure 10(a) shows raw reflectance images of the blood vessels of a mouse brain with multipositional illumination at 436 nm. We observed a non-uniform intensity across the images. That was because the light illumination was to one side of the imaging fiber so the tissue was not uniformly illuminated over the field-of view,

depending on the absorption and scattering properties of the tissue. We eliminated this by the subtraction of the inverse square function derived from a least square fitting as shown in Fig. 10(b) and used these for the following analysis.

The width of the blood vessels was obtained as shown in Fig. 11. The size of the ROI in the cross-correlation analysis was determined depending on the width of the blood vessel. (Blood Vessel Width (μm) and Size of ROI (μm^2) relationship as follows: 78 ≤, 209×209; 39–78, 104×104; 20–39, 52×52; <20, 26×26.). The shift value was obtained by cross-correlation analysis and the depth was calculated using the result of Experiment 1 as shown in Fig. 12. According to the analysis of the reflectance image of the OHP sheet, the absolute depth values could not be obtained correctly, but relative difference between them could be detected.

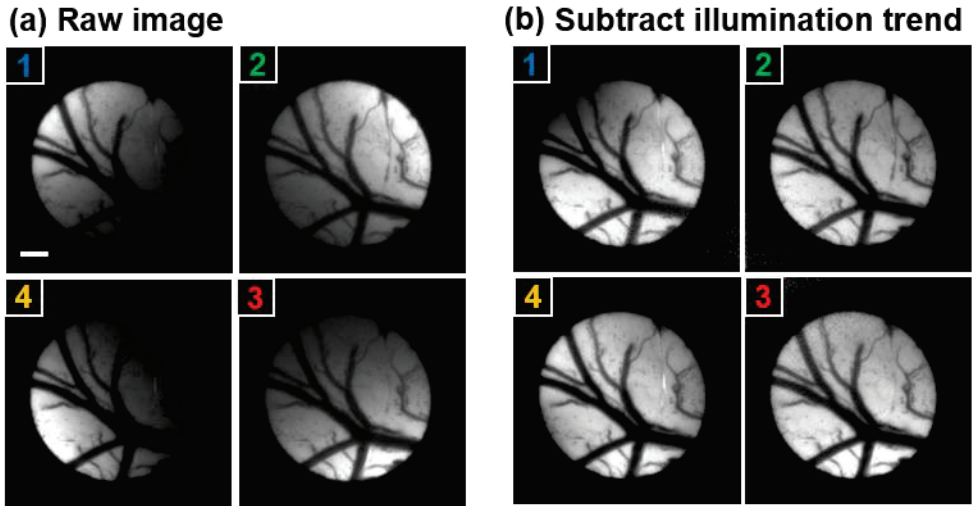

FIGURE 10. Reflectance images of mouse brain blood vessels with multipositional illumination (#1 to #4) at 436 nm. (a) Raw reflectance image. (b) Reflectance image with subtraction of illumination trend.

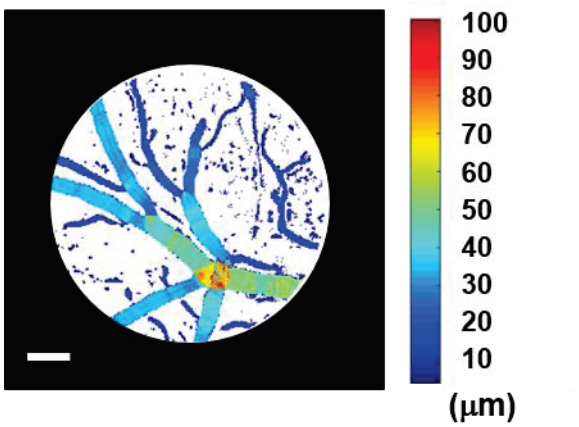

FIGURE 11. Width of the mouse brain blood vessels.

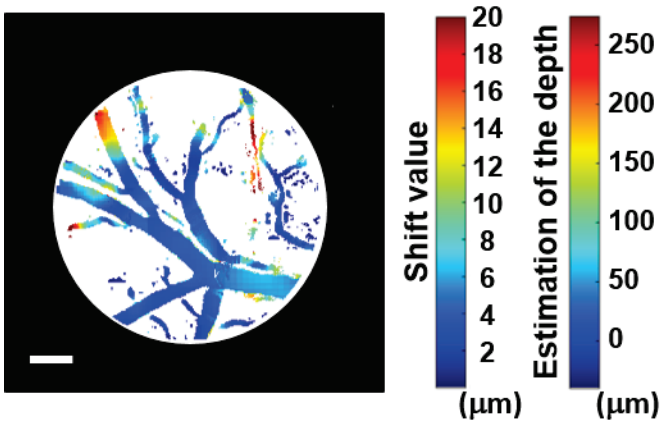

FIGURE 12. The vertical reconstruction (shift value and depth estimation) obtained by cross-correlation analysis of the reflectance image in Fig. 10(b). The color bars show the shift value and the depth estimation from the result of Experiment 1.

DISCUSSION

We measured reflectance imaging with a bundled-fiber-coupled endomicroscope with a multipositional illumination scheme and successfully demonstrated vertical reconstruction of the reflectance image by cross-correlation analysis. From Experiment 1 it became clear that the shift value changed linearly depending on the distance as shown in Fig. 7. The relative difference in depth was detected by cross-correlation analysis of the reflectance imaging of the OHP sheet (Fig. 9) and blood vessels (Fig. 12). However, properties of absorption and scattering of an agar gel are different from these of OHP sheet and tissue, so it was not possible to estimate the absolute depth value from the result of Experiment 1 (Fig. 7). Using a material which has similar properties to tissue's instead of agar gel with the target of a known or measurable depth (distance) in Experiment 1, the depth estimation of blood vessels could be estimated more precisely.

In this study, we adopted a simple miltipositional illumination scheme where illumination fibers were placed adjacent to the imaging fiber bundle. Therefore, the size of the end section was not small enough to insert into a site deep inside the body. Smaller diameter endomicroscopy systems allow the biomedical and clinical imaging of deep internal organs in minimally invasive way. Previously, a fiber-bundle reflectance imaging system using illumination through the imaging fiber itself without any additional illumination system has been introduced. [7-9]. Applying these techniques into a multipositional illumination scheme would be desirable for future study.

Optical techniques for three-dimensional surface reconstruction of endoscopes have been employed in clinical applications [10]. In this paper, we introduced a simple illumination scheme for micro-level reflectance imaging using a bundle-fiber-coupled fiber bundle enabling vertical reconstruction. We anticipate that future endocytoscopic application of this technique will facilitate the examination of particular areas in detail, and help to make optical biopsy a more effective alternative to histology. The advantage of our approach is the ability to produce live images along with three-dimensional information to visualize morphological features.

ACKNOWLEDGEMENT

This work was supported by Research Foundation for Opto-Science and Technology (to YA and RN), MEXT's "Program to Foster Young Researchers in Cutting-Edge Interdisciplinary Research" from MEXT/JST (to KK and RN), and by Grants-in-Aid for Scientific Research from the Japan Society for the Promotion of Science from MEXT/JSPS (26460294 to TS, 25135718 to KK, and 24590350 to RN and KN). RN was also supported in part by The Takeda Science Foundation and The Tatematsu Foundation. We thank Minako Matsuo (Toyohashi University of Technology) for technical support and Naobumi Kimura (Toyohashi University of Technology) for animal care.

REFERENCES

1. B. A. Flusberg, E. D. Cocker, W. Piyawattanametha, J. C. Jung, E. L. Cheung, and M. J. Schnitzer, "Fiber-optic fluorescence imaging," Nat Methods **2**, 941-950 (2005).
2. M. Hirano, Y. Yamashita, and A. Miyakawa, "In vivo visualization of hippocampal cells and dynamics of Ca2+ concentration during anoxia: feasibility of a fiber-optic plate microscope system for in vivo experiments," Brain Res **732**, 61-68 (1996).
3. A. D. Mehta, J. C. Jung, B. A. Flusberg, and M. J. Schnitzer, "Fiber optic in vivo imaging in the mammalian nervous system," Curr Opin Neurobiol **14**, 617-628 (2004).
4. D. Rector and R. Harper, "Imaging of hippocampal neural activity in freely behaving animals," Behav Brain Res **42**, 143-149 (1991).
5. M. Hughes, T. P. Chang, and G. Z. Yang, "Fiber bundle endocytoscopy," Biomed Opt Express **4**, 2781-2794 (2013).
6. T. Ohigashi, N. Kozakai, R. Mizuno, A. Miyajima, and M. Murai, "Endocytoscopy: novel endoscopic imaging technology for in-situ observation of bladder cancer cells," J Endourol **20**, 698-701 (2006).
7. M. Hughes, P. Giataganas, and G. Z. Yang, "Color reflectance fiber bundle endomicroscopy without back-reflections," J Biomed Opt **19**, 30501 (2014).
8. X. Liu, Y. Huang, and J. U. Kang, "Dark-field illuminated reflectance fiber bundle endoscopic microscope," J Biomed Opt **16**, 046003 (2011).
9. J. Sun, C. Shu, B. Appiah, and R. Drezek, "Needle-compatible single fiber bundle image guide reflectance endoscope," J Biomed Opt **15**, 040502 (2010).
10. L. Maier-Hein, P. Mountney, A. Bartoli, H. Elhawary, D. Elson, A. Groch, A. Kolb, M. Rodrigues, J. Sorger, S. Speidel, and D. Stoyanov, "Optical techniques for 3D surface reconstruction in computer-assisted laparoscopic surgery," Med Image Anal **17**, 974-996 (2013).